Faculty of Science and Technology (TNW)

Bachelor Thesis

Sudden bubble formation in carbonated drinks

B.M. de Gooijer

Date:
July 21, 2013

Examination Committee:
Prof. Dr. R.M. van der Meer
Dr. Ir. N.R. Tas
MSc O.R. Enriquez

UNIVERSITY OF TWENTE.

Foreword

This thesis is written as a completion to the bachelor Advanced Technology at the University of Twente. The bachelor programme is multidisciplinary covering topics in the field of mathematics, mechanics, electronics, physics, chemistry and business administration. In the search for a subject to reflect this multidisciplinary character I ended up at the Physics of Fluids group, a group which is studying various flow phenomena. What better can represent this Advanced Technology-character than the cosplay of fluid mechanics, physics and chemistry, known in the world of flows? When I found out the Physics of Fluids group especially focusses on flows related with bubbles, I made sure to find an assignment there. The world of bubbles and droplets has intrigued me since high school. My project to obtain a VWO diploma was on the stability of beer foams. Later, during the second year of my bachelor's program, a Lab on a Chip project on which I worked was titled 'Fabrication of PCR-droplets by means of a PDMS-microchip'. For this last stage in obtaining a bachelor's degree again the world bubbles and droplets is explored. This time in writing a thesis entitled 'Sudden bubble formation carbonated drinks'. I hope one will enjoy reading as much as I enjoyed writing.

Enschede, July 2013

Boukje de Gooijer

Abstract

Nowadays a lot of research is done on bubbles in champagne and beer. However research on the bubbles in the main ingredient of both beverages, namely water, is lagging behind. In this study daily conditions for carbonated water and their influence on the bubbles is examined.

The influence of temperature, shaking method, shaking time and resting time is related to the number of bubbles formed, their rising velocity and their growth rate.

The major outcome of this study is that the existing theory is not compatible with the found results. Carbonated water being opened unshaken at water temperatures between 15 and 35 °C shows larger radius growth rates than predicted by theory. The velocity with which the bubbles rises is in agreement with the theory. The range of water temperatures on his own does not lead to the overspilling of a bottle. Yet if the bottle in addition is shaken overspill is accomplished. Shaking using a vibrational generator at $10 - 50$ Hz cause the largest amounts of overspill for the whole temperature range. An increase in temperature causes an increase in number of bubbles formed for all shaking methods. Numbers of bubbles up to a maximum of 5500 are found when shaking using the vibrational generator.

Keywords: CARBONATED BEVERAGES, CARBON DIOXIDE, BUBBLE GROWTH

Contents

1 Introduction

All carbonated beverages are from a physical point of view interesting gas-liquid solutions. The presence of macromolecules such as sugar, proteins and ethanol determine for example the taste, color and if you might intoxicate yourself with a beverage. From the moment your drink is shaken to the moment you wet yourself by opening the bottle, the gas-liquid solution is known to experience a few different phenomena. What these phenomena are and how they contribute to bubble production is described in the first sections of this chapter. In the last section the influence of temperature, shaking method, shaking time and resting time on the number of bubbles formed, their rising velocity and their growth rate is proposed as the subject of this bachelor thesis.

The main beverage used in this study is carbonated water, in popular language also known as 'Spa red'. It is a liquid without any macromolecules, but with a large amount of dissolved CO_2. Before proceeding a division is made into three stages. The first stage is during the shaking of the bottle. In this stage the CO_2 is being entrained from the headspace of the bottle into the liquid. The second stage is between shaking and opening. In this stage the CO_2 is finding its way back to the headspace. The headspace can be reached in two ways, the CO_2 might rise to the top in a microbubble, or it can dissolve into the liquid and it reaches the headspace later by diffusing through the top surface. The last stage is after opening. In this stage the liquid becomes supersaturated with CO_2 by the sudden drop in pressure. Prior to opening the pressure in the headspace of the bottle is around $5 \cdot 10^5$ Pa while after opening the pressure becomes atmospheric pressure of about $1 \cdot 10^5$ Pa.

1.1 Supersaturation

Because supersaturation is the main reason for a gas-liquid solution to form bubbles the first section will describe this phenomena. As was described by Jones et al. [1] supersaturation is a quantification for the tendency of a system to produce bubbles. Supersaturation describes the excess of CO_2 molecules in the liquid compared to its equilibrium state. To quantify this excess of CO_2 molecules the supersaturation ratio is used. The supersaturation ratio SSR is defined by Lubetkin and Blackwell [2] as

$$\mathrm{SSR} = \mathrm{SR} - 1 \tag{1.1}$$

with SR the saturation ratio

$$\mathrm{SR} = \frac{c_L}{c_0} \tag{1.2}$$

where c_L is the concentration of dissolved CO_2 in the liquid bulk and c_0 is the equilibrium concentration corresponding to a partial pressure of gaseous CO_2 of atmospheric pressure.

The strive of a system to reach equilibrium is also used in Henry's law. Henry's law relates the partial pressure of a given gas above a solution to the concentration of the same gas dissolved into the solution. At constant pressure Henry's law can be expressed as follows

$$c = k_H P_{CO_2} \tag{1.3}$$

where c is the concentration of the dissolved CO_2 molecules, k_H is Henry's law constant and P_{CO_2} is the partial pressure of CO_2 molecules above the liquid. Henry's law constant for CO_2 at different temperatures can be calculated using

$$k_H(T) = k_H^\circ \exp\left[\frac{\Delta H_{\text{diss}}}{\mathcal{R}}\left(\frac{1}{T} - \frac{1}{298.15\ \text{K}}\right)\right] \tag{1.4}$$

where k_H° is Henry's law constant for solubility in water at 298.15 K, ΔH_{diss} is the dissolution enthalpy of CO_2 in water and $\mathcal{R}$ is the universal gas constant. Values for k_H° and $\frac{\Delta H_{\text{diss}}}{\mathcal{R}}$ were found on the website of the National Institute for Standards and Technology [3].

$$k_H^\circ = 0.34 \cdot 10^{-3}\ \text{mol/m}^3\ \text{Pa} \tag{1.5}$$

$$\frac{\Delta H_{\text{diss}}}{\mathcal{R}} = 2400\ \text{K} \tag{1.6}$$

According to J.P. Bas from Spa Monopole (personal communication, May 22-27, 2013) Spa Barisart 0.5 L bottles are carbonated during the filling process with 8 kg CO_2 per m^3 at a temperature between 15 and 20 °C. Using equation 1.4 and the constants as in equation 1.5 and 1.6 Henry's law constants for different temperatures can be calculated. Using Henry's law (1.3) the pressure in the headspace required to reach a concentration of 8 kgCO_2 per m^3 can be calculated. An overview of the calculated Henry's constants and required pressures is given in Table 1.1.

To calculate the supersaturation ratio at the moment the bottle of Spa Barisart is opened, a few steps have to be taken. The CO_2 in the headspace is assumed to behave as an ideal gas. This means that the pressure P, can be related to the number of moles n, the temperature T and the volume V via the universal gas constant $\mathcal{R}$ in the following relation

$$P = \frac{n\mathcal{R}T}{V}. \tag{1.7}$$

T [°C]	$k_H(T)$ [mol/m$^3 \cdot$ Pa]	$P_{CO_2}(T)$ [Pa]
15	$0.44 \cdot 10^{-3}$	$4.04 \cdot 10^5$
20	$0.39 \cdot 10^{-3}$	$4.66 \cdot 10^5$
25	$0.34 \cdot 10^{-3}$	$5.35 \cdot 10^5$
30	$0.29 \cdot 10^{-3}$	$6.11 \cdot 10^5$
35	$0.26 \cdot 10^{-3}$	$6.94 \cdot 10^5$

Table 1.1: Overview of Henry's law constants and required headspace pressures for different temperatures

To use this equation the volume of the headspace is required. This volume is calculated using MATLAB and comes down to

$$V_{head} = 31.1 \cdot 10^{-6} \text{ m}^3. \tag{1.8}$$

A more elaborate description of the used calculation can be found in Appendix A. The volume of the headspace is constant because it might be assumed that the water does not expand with small changes in temperature. The initial amount of CO_2 in the headspace n_i can now be calculated. For this calculation it is assumed that the water is bottled at 15 °C, the initial pressure at this temperature can be found in Table 1.1.

$$n_i = \frac{P_i \cdot V_{head}}{\mathcal{R} \cdot T_i}. \tag{1.9}$$

Using the principle of mass conservation the amount of CO_2 in the headspace at the time of the experiment (n_e) can be related to the initial amount of CO_2 in the headspace. This is expressed as follows

$$n_e - n_i = (c_{L,i} - c_{L,e}) \cdot V_L. \tag{1.10}$$

Here, V_L is the volume of the liquid of $0.5 \cdot 10^{-3}$ m^3, $c_{L,e}$ is the concentration of CO_2 in the liquid bulk at the time of the experiment and $c_{L,i}$ is the initial concentration of CO_2 in the liquid bulk of 181.8 mol/m^3 as was given by J.P. Bas from Spa Monopole. Combining equations 1.3, 1.9 and 1.10 the following expression is derived.

$$c_{L,e} = k_{H,e} \cdot \left[\frac{((c_{L,i} - c_{L,e}) \cdot V_L + n_i) \cdot T_e \cdot P_i}{n_i \cdot P_i} \right] \tag{1.11}$$

Solving this for $c_{L,e}$ gives the results as displayed in Table 1.2. The equilibrium concentration corresponding to a partial pressure of gaseous CO_2 of atmospheric

T_e [°C]	$c_{L,e}(T)$ [mol/m^3]	$c_0(T)$ [mol/m^3]	SSR [-]
15	181.8	45.6	2.99
20	180.5	39.5	3.57
25	179.1	34.4	4.20
30	177.6	30.2	4.89
35	176.0	26.5	5.63

Table 1.2: Dissolved CO_2 concentrations, equilibrium concentrations and supersaturation ratios for different temperatures at the time of the experiment

pressure can be calculated using Henry's law (1.3).

$$c_0(T) = k_H(T)P_{atm} \tag{1.12}$$

With $P_{atm} = 101325$ Pa and $k_H(T)$ is read from Table 1.1. An overview of the dissolved CO_2 concentrations, equilibrium concentrations and calculated supersaturation ratios at the time of the experiment can be found in Table 1.2.

1.2 Nucleation

Now it is known that the liquid is being made supersaturated by opening the bottle it is time to look at the next phenomena. Nucleation is the clustering of molecules which are in the same phase. So for example CO_2 molecules which cluster in water to form a bubble is a form of nucleation. But not all CO_2 molecules cluster all of a sudden when you open your drink. When a bubble is formed an interface between the CO_2 gas and the water must be created, this costs energy. On the other hand there is a gain in energy from the new volume that is created, the liquid wants the CO_2 molecules to get out it. So it depends on the surface to volume ratio of the bubble whether it is formed or not. When the release of energy of creating the new volume is enough to create the interfacial surface, the bubble will be formed. The radius at which there is sufficient energy to create the interface is called the critical radius. Liger-Belair [4] describe the critical radius as follows

$$R^* = \frac{2\gamma}{P_{\text{atm}} \cdot \text{SSR}} \tag{1.13}$$

in this equation γ is the surface tension of the liquid, P_{atm} is the atmospheric pressure and SSR is the supersaturation ratio. For the circumstances used in this research the critical radius is about 0.4 µm. The nucleation process of bubbles can be divided into four types.

Type I Classical homogenous nucleation

The characteristic of this type of nucleation is that there are no gas cavities present prior to the system being made supersaturated. Jones et al. [5] describe that a supersaturation ratio of 100 or more is needed for the nucleation to be of this type. In the case of carbonated beverages such as Spa Red the nucleation will not be of this type.

Type II Classical heterogenous nucleation

The difference with type I nucleation is that the process is catalyzed by the presence of another material. No gas cavities present prior to the system being made supersaturated, not in the liquid bulk, nor on the other materials' surface. Although the process is catalyzed, comparable supersaturation ratios as for type I are needed.

Type III Pseudo classical nucleation

For this type of nucleation pre-existing gas cavities are present. These gas cavities are in the liquid bulk or on another materials' surface. The radius of the gas cavities is smaller than the critical radius for bubble growth. After the liquid being made supersaturated local fluctuations in the supersaturation ratio cause these small cavities to grow, while others dissolve back into the liquid.

Type IV Non-classical nucleation

The last type of nucleation is one with pre-existing gas cavities larger than the critical radius for bubble growth. Because the gas cavities are already bigger than the critical radius there is no energy barrier to overcome and the bubbles will grow freely. The pre-existing gas cavities can both be in the liquid bulk and on another materials' surface. As was stated by Sahu et al. [6] this type of nucleation is responsible for spilling over a carbonated beverage.

1.3 Bubble rise and growth

After a bubble is formed it will go onto his journey across the liquid. During its journey the bubble experiences two forces which determine the velocity with which the bubble rises. The bubble wants to move upward due to a buoyancy force and will be slowed down by a drag force. The bubble will not only have a rising velocity, but also a velocity with which the radius grows. In this section both phenomena are described according to different theories. It is remarked that for a bubble to rise and grow in a liquid, the liquid does not have to be supersaturated. In other words, the bubbles might rise and grow during shaking, before opening and after opening.

Rising velocity as described by Epstein

Epstein [7] describes the terminal velocity for a bubble of radius R as follows,

$$v = \frac{g\rho}{3\eta}R^2. \tag{1.14}$$

Here g is the acceleration due to gravity, ρ is the density of the liquid and η is the viscosity of the liquid. When during shaking a bubble with $R \approx 5 \cdot 10^{-5}$ m is entrained in a 20 cm high bottle filled with water, the time it takes for a bubble to dissolve (t_{diss}) is the same as the time it takes for the bubble to reach the top surface (t_{rise}). So, larger bubbles will rise to the headspace, while smaller bubbles dissolve into the liquid. This causes more CO_2 to be in the liquid after shaking.

Rising velocity as described by Liger-Belair

Liger-Belair [4] uses the Stokes velocity multiplied by a numerical prefactor α to describe the velocity close to a glass wall. This α is smaller than 1 making it the bubble to be slower. This is due to the fact that the bubble is rising close to the glass wall. A non symmetric flow pattern due to a no stick boundary condition at the glass wall makes the bubble slow down. The velocity according to Liger-Belair is display in equation 1.15.

$$v = \frac{2\alpha g\rho}{9\eta}R^2. \tag{1.15}$$

Radius growth as described by Epstein

The main driving force for bubble growth is diffusion. Fick's law states that there is a flux from a high concentration to a lower concentration, the difference in concentration is proportional for the rate at which this process takes place. In the case of bubble formation in carbonated drinks this will cause the CO_2 going from the liquid into the bubble. The difference between the concentration of dissolved CO_2 in the liquid bulk c_L and in the close vicinity of the bubble surface in equilibrium with the gaseous CO_2 in the bubble c_{bubble} is thus proportional to the bubble growth. It is described by many [8], [4] that the concentration in the bubble can be calculated using Henry's law (equation 1.3) with the pressure in the bubble being approximated with the atmospheric pressure P_{atm}, therefore it holds that $c_{bubble} = c_0$. An expression for Δc can be found in the equation below. Values for c_L and c_0 at different temperatures can be found in Table 1.2.

$$\Delta c = c_L - c_0 \tag{1.16}$$

Epstein [7] describes the growth for a bubble at rest in an oversaturated liquid. The radius at time t is approximated by

$$R(t) = R_0\sqrt{1 + \frac{2\kappa_{rest}}{R_0^2}t} \tag{1.17}$$

with R_0 the initial bubble radius, and κ_{rest} the growth rate constant for a bubble at rest. This growth rate constant κ_{rest} is defined as

$$\kappa_{rest} = \frac{D\Delta c}{\rho_{CO_2}} \tag{1.18}$$

with D the diffusion coefficient, ρ the density of CO_2 and Δc the concentration difference as in equation 1.16. An overview of the calculated growth rate constants for a bubble at rest can be found in Table 1.3.

Radius growth as described by Liger-Belair

Liger-Belair [4] describes the growth for a bubble when rising through the liquid. The radius at time t is described by

$$R(t) = R_0 + \kappa_{rising} \cdot t \tag{1.19}$$

with R_0 the bubble radius when it detaches from its nucleation site and κ_{rising} the growth rate constant for a rising bubble. Theoretically κ_{rising} is described by

$$\kappa_{rising} \approx 0.63\frac{\mathcal{R}T}{P_{\text{atm}}}D^{2/3}\left(\frac{2\alpha\rho g}{9\eta}\right)^{1/3}\Delta c \tag{1.20}$$

with $\mathcal{R}$ universal gas constant, T the temperature in Kelvin, P_{atm} the atmospheric pressure, D the diffusion coefficient, α a numerical prefactor, ρ the density of the liquid, g the acceleration due to gravity, η the viscosity of the liquid and Δc the difference in concentration as in equation 1.16. Calculated values for κ_{rising} can be found in Table 1.3. Note that the growth as predicted by Liger-Belair is constant. Another expression for κ_{rising} is therefore

$$\kappa_{rising} = \frac{dR}{dt}. \tag{1.21}$$

1.4 Problem description

After describing the phenomena which occur prior to wetting yourself, still some questions around this process remain unanswered. Therefore, in this bachelor thesis the influence of temperature, shaking method and shaking time on the number of bubbles formed, their rising velocity and their growth rate is investigated. Furthermore it is investigated what number of bubbles must be formed and what their rising velocity and growth rate must be to make a bottle spill over.

T_e [°C]	$\kappa_{rising}(T)$ [µm/s]	$\kappa_{rest}(T)$ [µm^2/s]
15	414	6395
20	435	6734
25	454	7029
30	470	7286
35	485	7510

Table 1.3: Calculated growth rate constants for different temperatures

Lastly, the initial parameters are related to the amount of overspill and a resting time which should be taken to ensure dry clothing is deduced.

Shaking was done by hand, using a shaker and an ultrasonic cleaner. The bottles are shaken for different times and resting times, at different temperatures. High speed imaging is used to capture the process of bubble formation and growth. MATLAB is used to process the images.

2 Materials & Methods

Different brands and beverages were used to capture the process of bubble formation. The main type of beverage used in the experiments is Spa Barisart (generally sold), but also a lot of Quellbrunn (house brand of Aldi) bottles are used. The processes used to fulfill the different experiments are described in this chapter.

2.1 Setting the temperature of the bottles

The temperatures of the bottles were set by putting the bottles in a bucket filled with water and connected to a warm water bath. To overcome a difference in pumping and sucking speed of the water bath the bucket is placed at a higher water level and an extra tube from the bucket to the bath is added. A visualization of this setup is sketched in Figure 2.1. To ensure the experiment was done at the desired temperature, the water temperature was measured after each experiment using a digital thermometer.

2.2 Shaking the bottles

For this research the bottles were shaken in three different ways. First of all the bottles were shaken by hand. When the bottle is shaken by hand, the shaking time is approximately 30 seconds. Secondly the bottles were shaken using a vibration generator. The type of shaker used is a TIRA TV 50301. To shake the bottles using the shaker the bottle is placed in a tube and tightened using a piece of foam rubber. This setup is visualized in Figure 2.2. The vibration generator was used on two different amplitudes and frequencies. For an amplitude of $A = 2$ mm a frequency of $f = 50$ Hz is used. For an amplitude of $A = 10$ mm a frequency of $f = 10$ Hz is used. For these parameters Γ can be calculated using the formula,

$$\Gamma = \frac{A\omega^2}{g}, \text{ where, } \omega = 2\pi f.$$

For the used parameters of $A = 2$ mm and $A = 10$ mm, this corresponds respectively to a Γ of 20 and 4.

The last shaking method is by means of ultrasound. A Bransonic ultrasonic cleaner type 2510EMT is used to shake the bottles at a frequency of 42 kHz. The bottles where placed in the ultrasonic cleaner in two ways, standing up straight and laying in an angle. For all shaking methods there is a standard resting time of approximately 20 seconds. This is the time it takes to set the shaken bottles into the imaging setup.

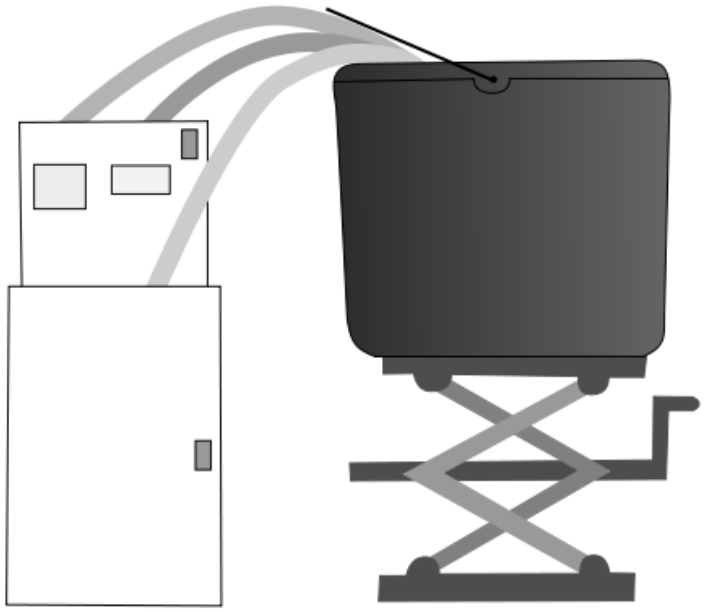

Figure 2.1: Side view of the setup used for warming the water bottles

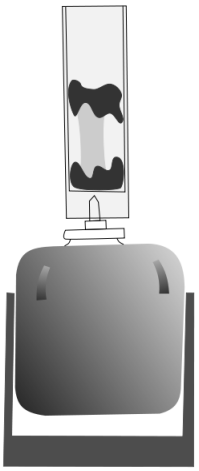

Figure 2.2: Side view of the setup used for shaking the bottles

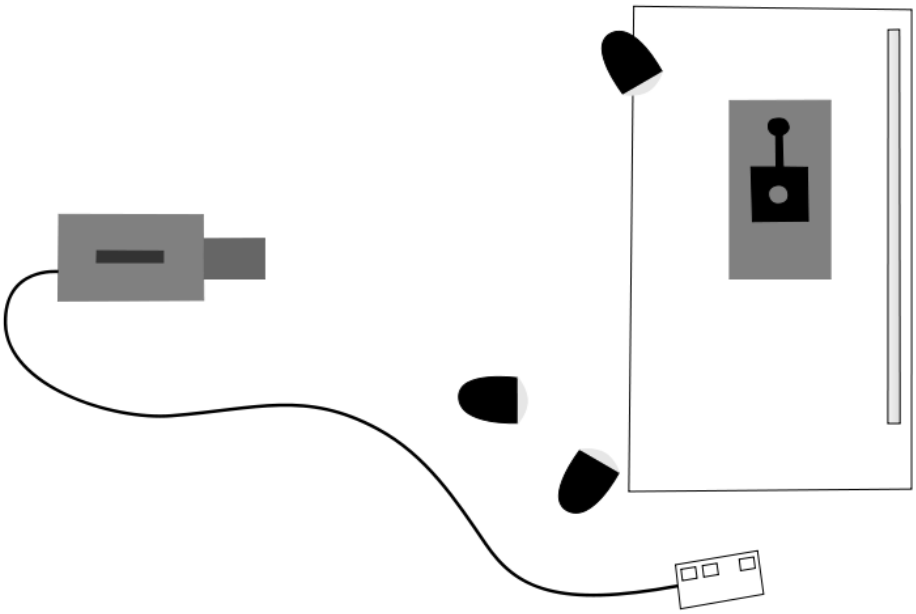

Figure 2.3: Top view of the setup used for imaging

2.3 Imaging

The high speed camera used in the experiments is a Photron-APX with a Carl Zeiss Makro-Planar 1:2.8 60 mm lens. The software used to save the images and view them later is Photron FASTCAM Viewer Ver.3.0. A remote controller is connected to the camera. The frame rate used in the experiments is 500 fps, the used shutter time is 1/6000 s. To ensure sufficient lightning three halogen lamps are used, which are placed as shown schematically in Figure 2.3. To prevent the camera from wetting the bottle is placed in a larger glass container displayed by the large rectangle in Figure 2.3. To ensure bright pictures a clean white plastic plate is placed to the back of this container. The bottle is placed on a piece of sandpaper and clamped to prevent it from twisting. To uncap the bottles as fast as possible a drilling machine is used. This drilling machine is provided with cap opener made of teflon. This cap opener has a cylindrical top part which is placed over the cap. To secure a tight fit the teflon is surrounded with a messing ring. A drawing of the cap opener can be found in Figure 2.4.

Before and after the images were taken the weight of the bottle including the cap is measured with a Denver instrument scale. The time it took to place a bottle in the setup for imaging was measured using a stopwatch.

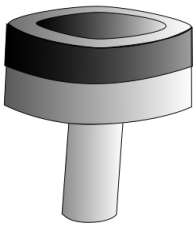

Figure 2.4: Device used to open the caps

2.4 Image processing

To process the images MATLAB R2013a is used. The image is converted to black and white in a few steps. To clarify the steps a sample of 9 different experiments is taken and displayed in Figure 2.5. The first step is to load the images in MATLAB. The second step is to subtract the background from the original images. The bubbles are now lighter than the background. The last step is to set all bubbles to white pixels (ones) and the background to black pixels (zeros). An image in ones and zeros is called a binary image and MATLAB is now able to process it. Information such as bubble size, frame number and x- and y-coordinates of the bubble's centroid are stored in a matrix. After the analysis is done MATLAB removes the image and loads the next image. A more elaborate description of the MATLAB-scripts can be found in Appendix A.

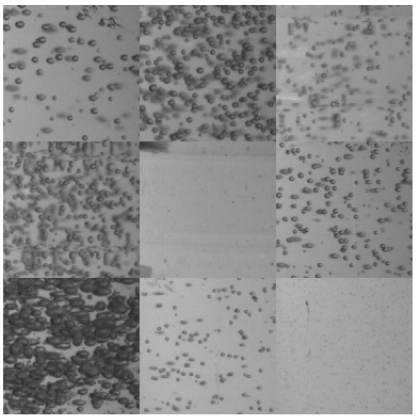

Step 1: Sample images

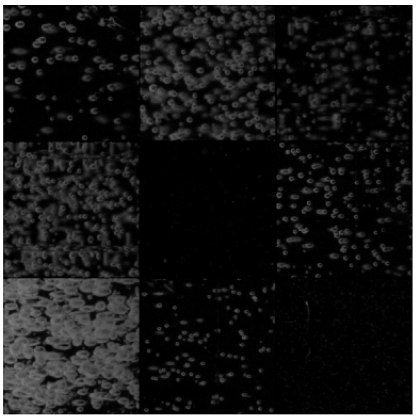

Step 2: Sample images without background

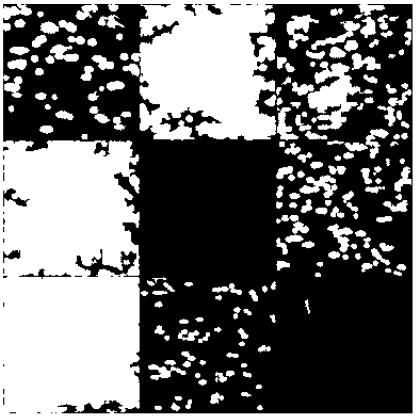

Step 3: Sample images in black and white

Figure 2.5: Steps in conversion from a grey scale image to a black and white image

3 Results

The results from this study are divided into three parts. The first part is about the effect of several parameters on the spill over amount. The section part describes the effects for the same parameters on the number of bubbles formed and lastly the effects on rising velocity and growth are covered.

3.1 Effects on the spill over amount

The effect of ultrasonic shaking on canned beer is described by Sahu, et al [6]. They report large amounts of spill over for canned beer which is shaken at 28 kHz. As can be seen clearly in Figure 3.1 ultrasonic shaking appears to have no effect on carbonated water. The bottles which were shaking ultrasonically (denoted o) overflow the same amount as unshaken bottles (denoted $\cdot$). Shaking by hand (denoted *) appears to have very little effect at lower temperatures. However at temperatures higher than 30 °C a reasonable amount of over flow is reached. The largest amount of over flow is generally reached when shaking the bottle using the vibration generator (denoted ∇).

3.2 Effects on the number of bubbles formed

What appears clearly from Figure 3.2 is that shaking using a vibration generator (denoted ∇) produces a large amount of bubbles. Generally speaking an increase in temperature results in an increase in the number of bubbles formed. As in the amount of over spill, ultrasonic shaking (denoted o) has comparable effects with not shaking (denoted $\cdot$) also in the number of bubbles formed. Lastly Quellbrunn water (denoted in blue and aqua) seems to produce a larger number of bubbles for the same temperature and shaking method than Spa water (denoted in red and orange).

The experiments in which a reliable number of bubbles were found for shaking using the vibration generator, were all performed around a temperature of 20 °C. Although the temperature was constant the experiments were performed using different frequencies, amplitudes, shaking times and resting times. For that reason the data points for the vibration generator is plotted a second time in Figure 3.3. A resting time of 60 seconds (denoted in orange) decreases the number of bubbles drastically. The shaking time does not influence the number of bubbles formed. Also a different frequency and corresponding amplitude (denoted $\cdot$ for $f = 10$ Hz and denoted * for $f = 50$ Hz) do not influence the number of bubbles formed.

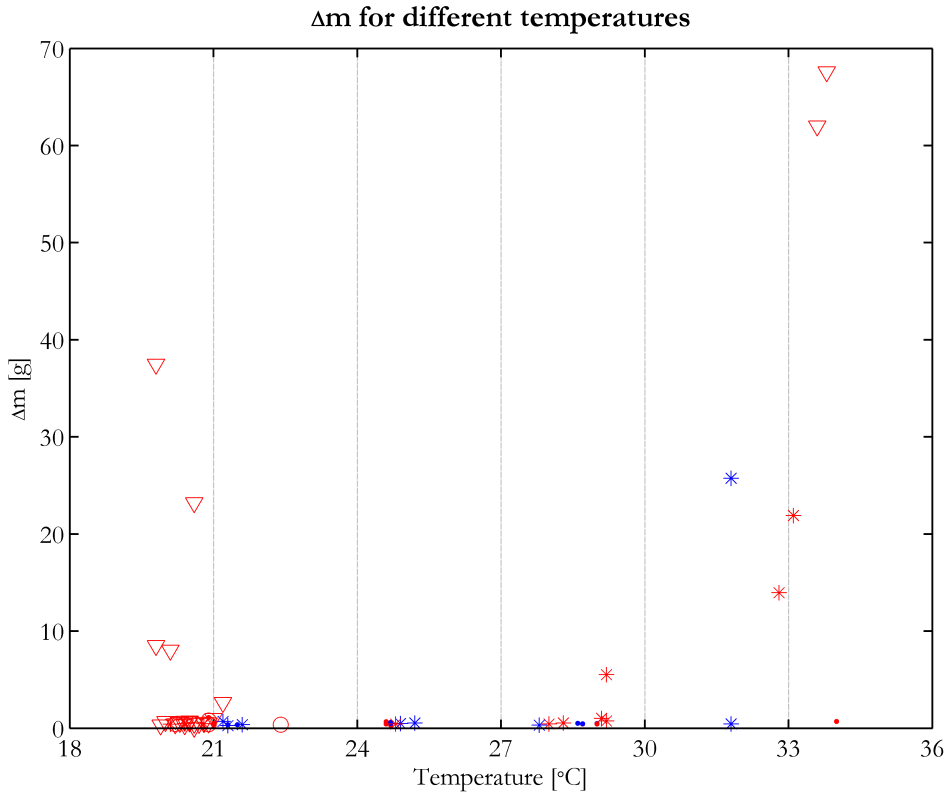

Figure 3.1: Plot of the change in mass before and after opening the bottle at different temperatures. The bottles where shaken in various ways denoted as the symbols below. Two brands of carbonated water were used denoted as the color of the data point.

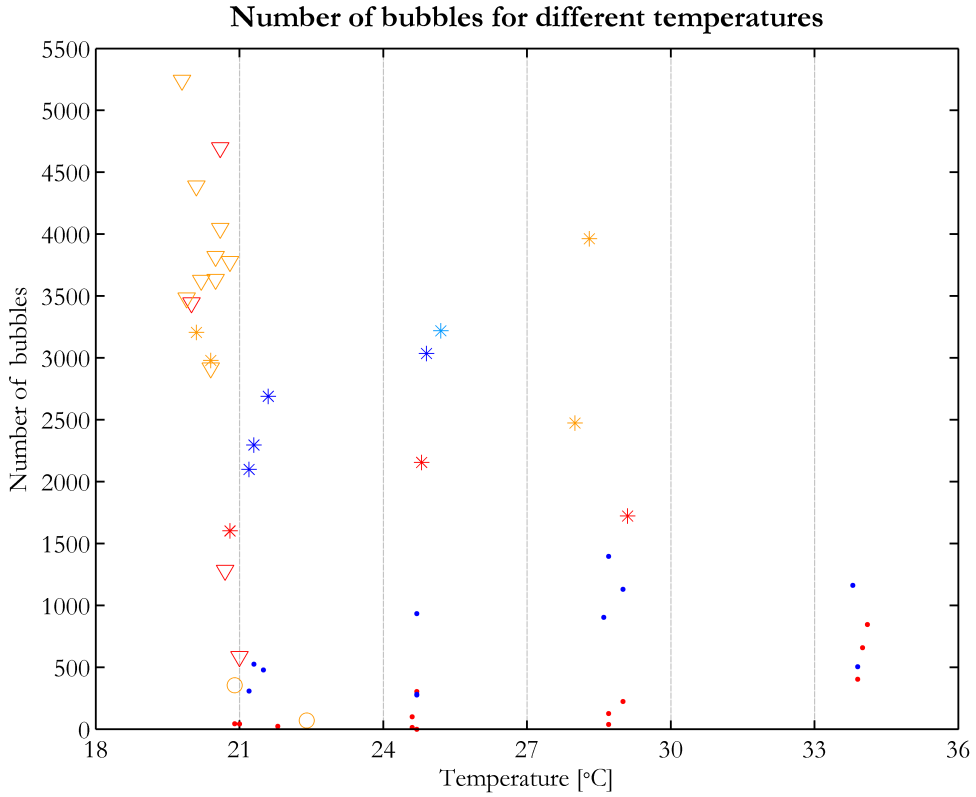

Figure 3.2: Plot of the number of bubbles formed for different temperatures. The bottles were shaken in various ways denoted as the symbols below. There was made a distinction between visually reliable data points denoted in a darker color and less reliable data points denoted in a lighter color.

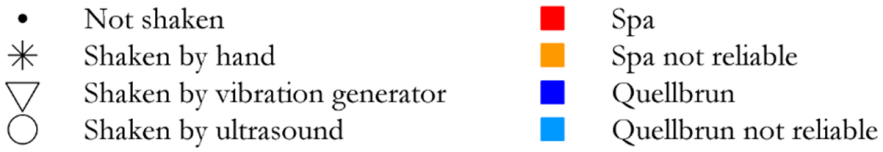

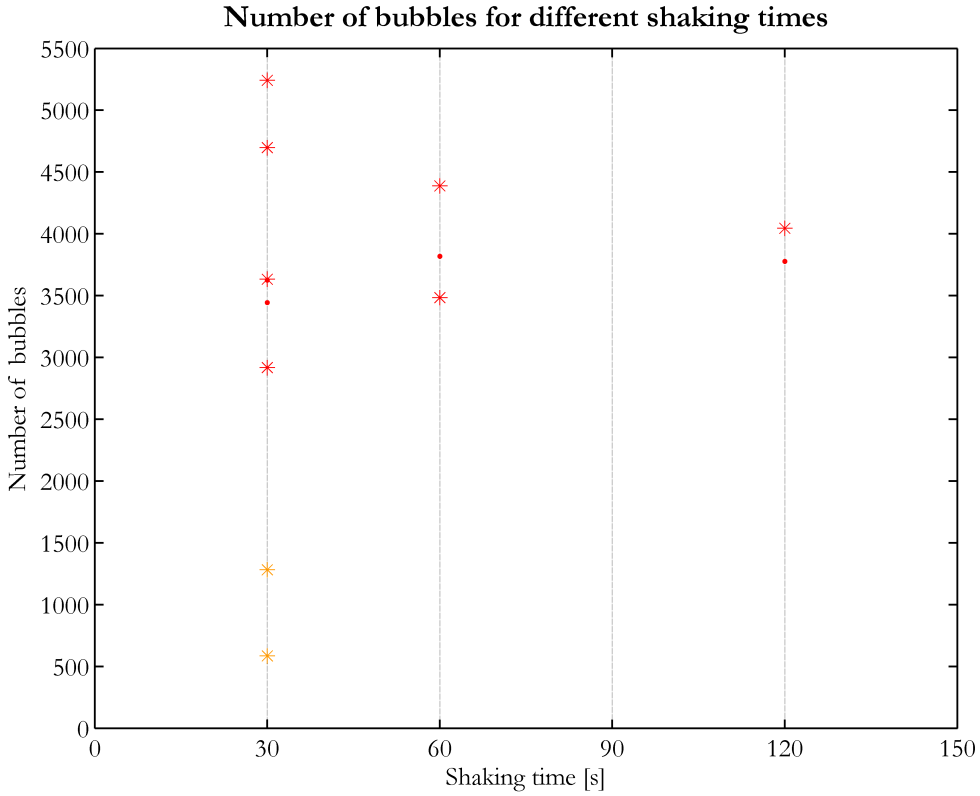

Figure 3.3: Plot of number of bubbles formed when using a vibration generator for different shaking times. The vibration generator is used for different frequencies with corresponding amplitudes denoted as the symbols below. The experiments were performed using two resting times denoted as the color of the data point.

T (°C)	$\frac{ds}{dt}$ (m/s)	$\frac{dR}{dt}$ (µm/s)
20.3	0.279	5200
20.7	0.278	4600
24.8	0.235	6500
26.4	0.278	7000
33.8	0.249	7600
33.5	0.307	14700

Table 3.1: Overview of experimental averaged rising velocities and growths at different temperatures

3.3 Effects on rising velocity and growth

The results for the effects on rising velocity and growth are only found for unshaken Spa water. The terminal velocity using an average radius of 0.3 mm is calculated using equation 1.14 and turns out to be 0.3 m/s. This matches the results as can be seen in Table 3.1.

The rate with which radius grows is larger in the experiments compared to the theory. The experimental results for κ_{rising} are 10 to 15 times as big as would be predicted by the theory of Liger-Belair (see section 1.3). Also the theory as described by Esptein (see section 1.3) does not match the obtained results. In Figure 3.4 the growth for three bubbles at two different temperatures is plotted. The experimental data (denoted in blue) shows a linear growth, but the slope for all bubbles at all temperatures is much steeper than the theoretical growth. For the same parameters as used in the experiments, the bubble growth as predicted by Epstein (denoted in dark red) appears to be negligible. Also the growth as predicted by Liger-Belair (denoted in light red) is much smaller than the experimental growth.

The difference between the growth as predicted by Liger-Belair and the experimental growth is explored further in Figure 3.5. To compare the bubble growth at different temperatures the radius at time t is subtracted with its initial radius $R0$, also the temperature dependency is canceled by dividing by the temperature T at which the experiment was the performed and the concentration difference Δc between the liquid bulk and the bubble. According to the theoretical bubble growth (denoted in black) as described in equation 1.20 the slope of the graph should show no more temperature dependency. However if Figure 3.5 is examined closely the experimental growth rates do increase with temperature. Also none of the bubbles' growth trajectories (denoted with o, for different temperatures) is comparable to the theoretical growth.

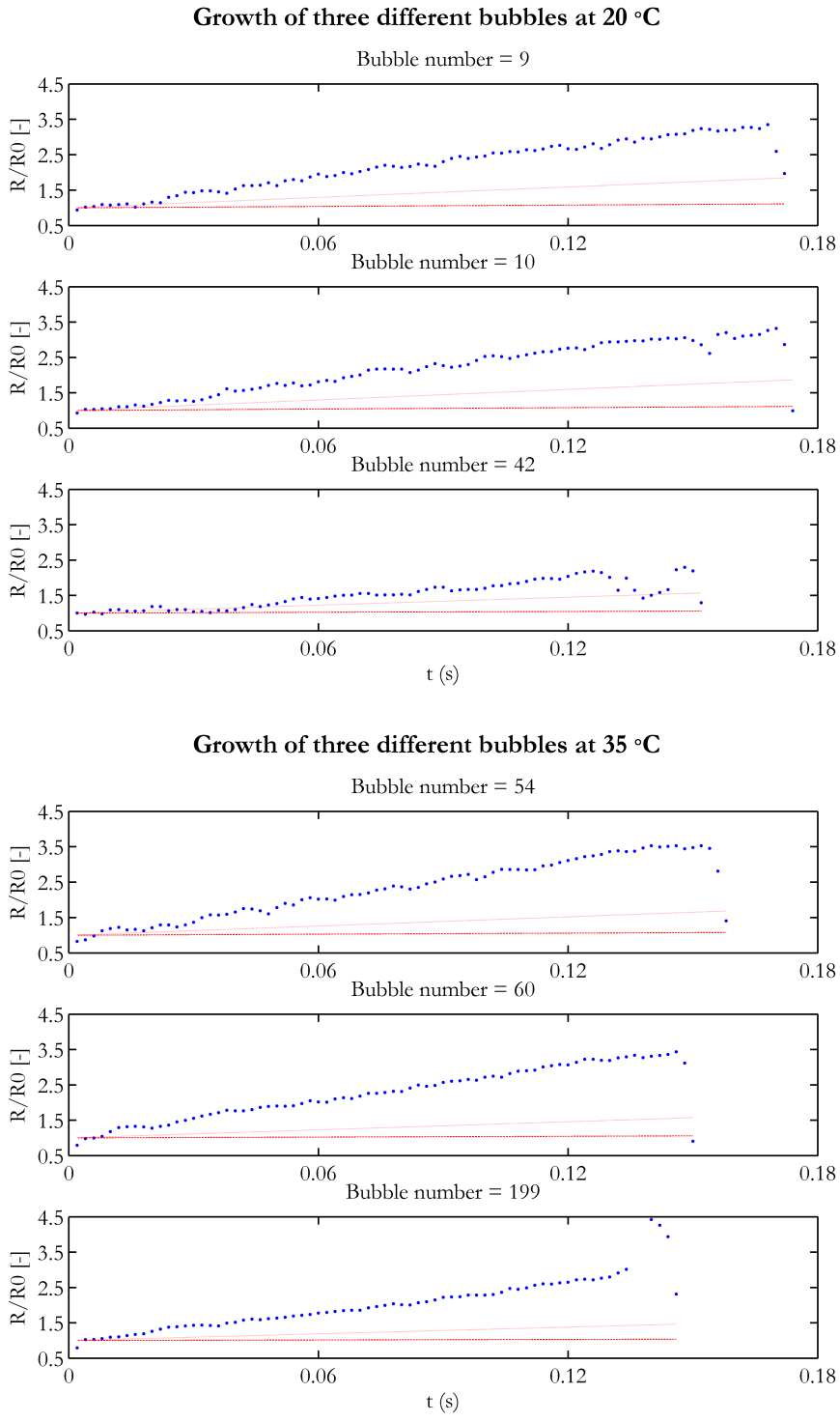

Figure 3.4: Plots of the growth in the dimensionless radius for three different bubbles at two different temperatures. Bottles were not shaken prior to opening them. The experimental data is denoted in blue, the theoretical radius growth as described by Liger-Belair is denoted in light red and the theoretical radius growth as described by Epstein is denoted in dark red.

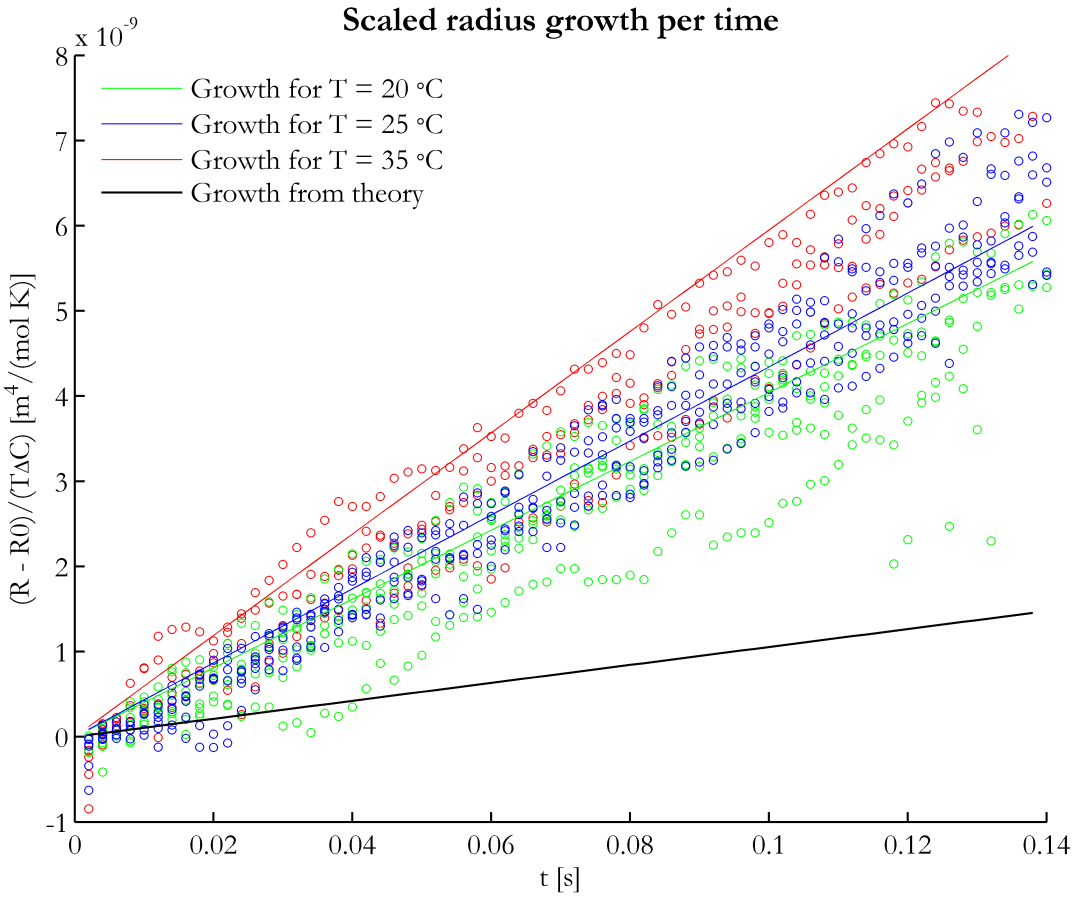

Figure 3.5: Radius growth scaled by subtracting the initial radius (R0) and dividing by the temperature (T) and the concentration difference (Δc) to make it independent of temperature. Experimental data are for different temperatures denoted in the color of the data point. Theoretical growth in plotted in black.

4 Discussion

When examining the results of this study a few remarks can be made. The subjects to be discussed are divided in the same parts and sequence as the results.

4.1 Discussion on the spill over amount

The results described by Sahu, et al [6] are obtained using canned beverages. The water used in these experiments was packed in plastic bottles, this might have influenced the shaking. Other explanations why less overspill was reached for these experiments are that longer resting times are used, the uncapping process took longer, the water contained no macromolecules and that the experiments were performed at a 1.5 times higher frequency.

The overall low amounts of over spill which are found can be explained by the unintentional resting times used for all experiments. As soon as the bottle had to be placed in the imaging setup a resting time of about 8 seconds was needed. For the ultrasonic shaking and shaking using the vibrational generator an extra resting time of about 12 seconds was needed to place the bottle in the imaging setup. Because there is no exact data on the resting times it is difficult to say something about the microbubble distribution as described by Sahu, et al [6].

4.2 Discussion on the number of bubbles formed

The number of bubbles for higher temperatures could rarely be deduced from the taken images. However the numbers that where found are comparable to the numbers that where found by Lubetkin and Blackwell [2]. This reason that few results were found for higher temperatures was that a large number of pre-existing gas cavities was present in the liquid bulk which grew very rapidly. When the bubbles started touching each other it was not possible anymore to filter one bubble from the other. To support this difficulty one might take a look at Figure 2.5. For a human eye separate bubbles can be distinguished, however it was not managed to write a computer program which could do the same. Difficulties found when trying to process the images are the following:

- The lightning was not set properly even. This resulted in an uneven background, in the bottom part of the bottle the bubbles appeared darker than the background while in the top part of the bottle the bubbles appeared lighter than the background.

- The bubbles have different radii over time or are not even round at all. The change in shape with the uneven background combined, made it impossible

to search for a specific pattern as bubble. Bubbles start as a sphere with a reflection from the lightning from the top and end ellipsoidal or kidney-shaped at the top with a reflection from the lightning from below.

- Due to the spherical geometry of the bottle bubbles also rise before or after the focal length of the lens. This results in blurry images.

4.3 Discussion on the rising velocity and growth

The growth rates as predicted by Epstein [7] and Liger-Belair [4] mismatches the data found in the experiments. For the Epstein growth the mismatch can be explained by the bubbles in the experiment rising through the liquid, while the theory is designed for bubbles at rest. The movement through the liquid makes more CO_2 available for the bubble to grow. Furthermore the Epstein growth is based on a situation without convection, while in the experiments there was convection.

The theoretical growth rate as described by Liger-Belair is determined for champagne and beer 3 minutes after pouring. The growth rates found in this setup are for water the moment the bottle is opened. This difference in time after opening might cause a sufficient change in the liquid bulk concentration of CO_2 in carbonated water to slow down the growth rate of the bubbles to values found by Liger-Belair.

The Liger-Belair growth might also mismatch due to the fact that not all bubbles are perfectly round. A sphere has the smallest surface to volume ratio, meaning a kidney-shaped bubble will have more area available for diffusion than a sphere. This will result in a higher growth rate. However for the bubbles plotted in Figure 3.5 the areas where round. The theory of Liger-Belair for the growth rate describes no temperature dependence when the radius is divided by the concentration difference and the temperature. However Figure 3.5 does show an increasing slope for an increasing temperature. This might be explained by a small temperature dependency which is still left in the diffusivity constant and the density and the viscosity of water. The diffusivity constant increases with increasing temperature resulting in a larger κ_{rising}, the density of water decreases for increasing temperature resulting in a smaller κ_{rising}, lastly the viscosity decreases for increasing temperatures resulting in a larger κ_{rising}.

Lastly water is different from champagne and beer due to the absence of macromolecules. Macromolecules are reported to accumulate on the surface of a bubble and making it become more rigid by Liger-Belair. This more rigid bubble might hinder the growth in two ways. The diffusion process is slower because surface area is occupied by macromolecules or the macromolecules form a sort of shell around the bubble making it harder to expand.

5 Conclusions

Based on the outcomes of this study conclusions on several subjects may be drawn. The structure of this chapter is proceeded as in the previous two chapters.

5.1 Conclusions on the spill over amount

A high temperature on its own does not cause a bottle of carbonated water to overflow. For a bottle to overflow it needs to be shaken either by hand or by a vibration generator. When a bottle is shaken by hand a temperature of around 30 °C is needed for the bottle to overflow. Shaking using a vibration generator cause the bottle to overflow, independent of the temperature and shaking time. The resting time which should be taken to ensure no over flow is not been determined, because generally a bottle does not over flow. Instead of making a bottle overflow ultrasonic shaking seems to degas carbonated water. A conclusion on the rising velocity and growth rate necessary to make a bottle overflow can not be drawn based on the results. However visually it was determined that a large number of bubbles with great growth rates cause a bottle to overflow.

5.2 Conclusions on the number of bubbles formed

A relation is found between an increase in temperature and the number of bubbles formed for shaken and unshaken bottles. Shaking using a vibration generator results in the largest number of bubbles. For higher temperatures no conclusions can be drawn on the number of bubbles formed using a vibration generator. However, following the trend for the unshaken and by hand shaken results, a bottle shaken by the vibration generator would form even larger numbers of bubbles. Bottles shaken by ultrasound show comparable or even lower results than unshaken bottles. For bottles shaken by vibration a larger shaking time has no influence on the number of bubbles formed. Increasing the resting time to 120 s for a bottle shaken by vibration minimally halves the number of bubbles formed.

5.3 Conclusions on the rising velocity and growth

An increase in temperature does not change the velocity with which the bubble rises through the liquid. An increase in temperature does result in a larger radius growth constant. A conclusion on the influence of shaking method and shaking time can not be drawn because only results could be deduced for unshaken bottles.

6 Recommendations

For further research there are a few topics on which I would like to suggest some improvements. The structure in which these topics are presented is the same as in the prior chapters.

6.1 To determine the spill over amount

To determine the parameters which result in a overspill more extensively, I recommend improving the setup. In the used setup bottles could not be shaken and opened fast enough. Besides that bottles were placed differently in the imaging setup every experiment, this meant that they could be standing up straight but also be in a small angle. I suggest using a rectangular test sample which can be shaken, opened and imaged within the same setup. This will give better control over the shaking and resting times. In this study there is no elaboration on the effect of the frequency with which the bottles are shaken. Comparing the results for shaking using the vibrational generator ($10 - 50$ Hz) and the ultrasonic cleaner (42 kHz) with the results obtained by Sahu, et al. [6] suggest that this might be an interesting research topic.

6.2 To determine the number of bubbles formed

As suggested in the previous section, using a rectangular test sample will also benefit the determination of the number of bubbles formed. A thin cubic test sample can be lightened more even and will cause all the bubbles to flow at the focal length of the lens. Another way to determine the number of bubbles formed is described by Lubetkin [2]. In his research the sound of the popping bubbles at the top surface is used to determine the number of bubbles formed. The disadvantage of this method that it is not suitable for counting bubbles when the bottle overflows.

6.3 To determine the rising velocity and growth

The results of this study for the bubble growth in carbonated water are not compatible with the existing theory. Determining the rising velocity and growth will also benefit from a rectangular test sample by being able to track the bubbles better. For further research I suggest doing more experiments with unshaken water in an improved setup. Further investigations on the bubble growth longer times after opening are needed to compare to the theory. To rule out any effects of the shape of the bubble on the growth rate it is suggested writing a MATLAB code to check the roundness of the bubble. This might be done using the

'MajorAxisLength' and 'MinorAxisLength' options in regionprops. For this study only the 'Centroid' and 'Area' options are used. The current study did not succeeded in drawing any conclusion on the effects of shaking on the bubble's rising velocity and growth. Therefore more research in an improved setup with shaken samples is recommended. In this study there is no research done at the effects of the present minerals. These minerals might have an effect on the water itself and on macromolecules, influencing the bubble growth.

7 Acknowledgements

Some people contributed in one way, or another to the writing of this thesis. I am grateful to be surrounded with those people and would therefore take the ability to thank them.

Devaraj van der Meer
for his scientific input, time and smile.

Niels Tas
for comming back to the University of Twente for me to be able to graduate.

Oscar Enriquez
for the freedom in doing this thesis and his clear understanding of the world of bubbles.

Haico Stegink
for letting me write my thesis very peacefully and being able to read my thesis while I sleep due to time difference.

Luuk van der Velde
for pushing me to write this thesis in LaTeX and for providing me with helpful input on the logic of my MATLAB scripts.

Mathijs Bronkhorst
for providing me with his experience with image processing in MATLAB.

All the girls from my sorority Spooky because I do not want to thank only men.

Bibliography

[1] S. F. Jones, G. M. Evans, and K. P. U. Galvin, "The cycle of bubble production from a gas cavity in a supersaturated solution," *Advances in Colloid and Interface Science*, vol. 80, pp. 51–84, 1999.

[2] S. Lubetkin and M. Blackwell, "The Nucleation of Bubbles in Supersaturated Solutions," *Journal of Colloid and Interface Science*, vol. 26, no. 2, pp. 610–615, 1988.

[3] R. Sander. (2011) Carbon dioxide. [Online]. Available: http://webbook.nist.gov/cgi/cbook.cgi?Formula=CO2&NoIon=on&Units=SI&cSO=on

[4] G. Liger-Belair, "The physics and chemistry behind the bubbling properties of champagne and sparkling wines: a state-of-the-art review." *Journal of agricultural and food chemistry*, vol. 53, no. 8, pp. 2788–2802, Apr. 2005. [Online]. Available: http://www.ncbi.nlm.nih.gov/pubmed/15826021

[5] S. F. Jones, G. M. Evans, and K. P. U. Galvin, "Bubble nucleation from gas cavities - a review," *Advances in Colloid and Interface Science*, vol. 80, pp. 27–50, 1999.

[6] K. K. Sahu, Y. Hazama, and K. N. Ishihara, "Gushing in canned beer: the effect of ultrasonic vibration." *Journal of colloid and interface science*, vol. 302, no. 1, pp. 356–362, Oct. 2006. [Online]. Available: http://www.ncbi.nlm.nih.gov/pubmed/16793054

[7] P. Epstein and M. Plesset, "On the Stability of Gas Bubbles in Liquid-Gas Solutions," *The Journal of Chemical Physics*, vol. 18, no. 11, pp. 1505–1509, 1950. [Online]. Available: http://link.aip.org/link/?JCPSA6/18/1505/1

[8] C. G. J. Bisperink and A. Prins, "Bubble growth in carbonated liquids," *Colloids and Surfaces A: Physicochemical and Engineering Aspects*, vol. 85, pp. 237–253, 1994.

A Elaboration on MATLAB

Calculating the volume of the headspace

To calculate the volume, the headspace is divided into two parts. The first part is from the water surface ($h0$) to the part where the screw-thread begins ($h1$) and is described by a parabola. The second part is the part with screw-thread to the top of the bottle ($h2$) and is described by a cylinder. The different heights are measured using the `imdistline`-tool in MATLAB. By measuring the diameter of the seal with a ruler and with the `imdistline`-tool in MATLAB it follows that 1 cm is approximately 350 pixels. Then h_0, h_1 and h_2 are respectively $0, 400$ and 1200 pixels.

For part 1 the radius in pixels is described as follows,

$$r = 800 - \frac{400}{160000}h^2 \tag{A.1}$$

The volume of part 1 is calculated by taking the integral from h_0 to h_1. To get the volume in centimeters the volume in pixels is divided by 350^2.

$$V_{part1} = \frac{1}{350^2}\int_{h_1}^{h_0} 2\pi r\, dh = 13.7 \text{ cm}^3 \tag{A.2}$$

The volume of part 2 is calculated by taking the integral from $h1$ to $h2$ over constant r of 400 pixels.

$$V_{part2} = \frac{1}{350^2}\int_{h_2}^{h_1} 2\pi r\, dh = 16.4 \text{ cm}^3 \tag{A.3}$$

The total headspace is given by adding the volumes of both parts.

$$V_{headspace} = V_{part1} + V_{part2} = 31.1 \text{ cm}^3 = 31.1 \cdot 10^{-6} \text{ m}^3 \tag{A.4}$$

Determining the size of each bottle

The bottles of Quellbrunn and Spa water are depicted in different sizes every day experiments were performed. To get the average number of pixels the bottles are depicted in, an average is taken of multiple experiments at one day. In table A.1 an overview of the average different bottle sizes per day can be found.

Converting an image to black and white

To convert the image to black and white a few steps are taken. At first the background of the image is found. This is done by taking a sample of 50 frames out

Date	Brand	Number of pixels
15-5-2013	Spa	261457
	Quellbrunn	227856
16-5-2013	Spa	259488
	Quellbrunn	233801
27-5-2013	Spa	272667
	Quellbrunn	250278
28-5-2013	Spa	264327
29-5-2013	Spa	268704

Table A.1: Overview of different bottle sizes

of the sequence of images from the experiment. For the background the median of these 50 frames is taken. To convert the image to black and white the original image is subtracted from the background. Then a level of 10 is set to assign black or white to a pixel. Pixels which have a larger value than 10 are assigned to be white and pixels which have a lower value than 10 are assigned to be black. The actual code can be found below.

```
fileFolder = fullfile(datapath, date, experiment);
path(fileFolder, path)
dirOutput = dir(fullfile(fileFolder,'a*.tif'));
fileNames = {dirOutput.name}';
numFrames = numel(fileNames);

testimage = 250;
I = imread(fileNames{testimage}); %original image
si = size(I);

%find background of image
sample_rate = floor(linspace(1, numFrames, 50));
sample_back = zeros([length(sample_rate) si(1) si(2)],'uint8');

for nback = 1:length(sample_rate)
    tback = sample_rate(nback);
    img = imread(fileNames{tback});
    sample_back(nback,:,:) = img;
end

m_sample_back = uint8(median(sample_back));
back = reshape(m_sample_back,h,w);
```

```
filt = fspecial('disk', 1);
back = imfilter(back, filt);

%convert image to black and white
I_noback = back - I;

level = 10;
BW = I_noback > level;
BW = bwareaopen(BW, 20);
BW = imfill(BW,'holes');
```

Calculating the average velocity

To calculate the rising velocities of the bubbles the x- and y-coordinates are differentiated, squared and added. After that the square root is taken and the result is divided by the elapsed time. To convert the velocity from pixels per frame to meter per second it is multiplied by the frame rate and a conversion factor. This conversion factor was found by marking a bottle with a line of 2 cm and relating it to the number of pixels in an image.

```
pixtom = 2e-2/512; %m/pix
framerate = 500; %fps

dt = (length(frames) - 1)/framerate;
dx = diff(xlocs);
dy = diff(ylocs);
ds = sqrt(dx.^2 + dy.^2)*pixtom;

vavg = sum(ds)/dt;

vavgs{eCount,1} = experiment;
vavgs{eCount,2} = vavg*pixtom*framerate;
```

Calculating the average growth

The trajectories of all bubbles were filtered. This was done to eliminate very short tracks or tracks in which two bubbles are seen as one. After the trajectories were filter the average growth was calculated by divinding the area by π and taking square root. The filtering and calculation was done using the following code.

```
pixtom = 2e-2/512; %m/pix
framerate = 500; %fps

```

```
4  for label = 1:nlabels
5
6      oldareas = sBubbles{label,8};
7      doldareas = diff(oldareas);
8
9      minval = -25;
10     maxval = 50;
11     ind = find(doldareas > maxval | doldareas < minval, 1, ...
           'first');
12
13     if ind == 1
14         disp([num2str(label) ' Bubble is too big'])
15         continue
16     end
17
18     if isempty(ind)
19         cutoldareas = oldareas(2:end);
20     else
21         cutoldareas = oldareas(2:ind-1);
22     end
23
24     cuttend = length(cutoldareas);
25     cutt = [1:cuttend];
26
27     ndt = floor(cuttend/3);
28     if ndt < 2
29         disp([num2str(label) ' Too few data points'])
30         continue
31     end
32     newt = linspace(2,cuttend,ndt);
33     newareas = spline(cutt, cutoldareas, newt);
34     newRs = sqrt(newareas./pi);
35
36     dnewRs = diff(newRs);
37     dRdt = sum(dnewRs)/length(dnewRs);
38
39     lcount = lcount + 1;
40     dRdts{lcount,1} = label;
41     dRdts{lcount,2} = dRdt;
42     dRdts{lcount,3} = dnewRs;
43 end
44
45 gavgexp = sum([dRdts{:,2}])/length(dRdts(:,2))
46
47 gavgs{eCount,1} = experiment;
48 gavgs{eCount,2} = gavgexp*pixtom*framerate;
```

A more rigorous method to calculate the radius growth is shown below. This method is only used for a selection of bubbles from which the trajectory was checked by a human eye.

```
RPix = sqrt(areasPix./pi);
R = RPix(1:end-15)*pixtom;
smoothR = smooth(R,10,'rlowess');
dRs = diff(smoothR);
dt = (length(frames) - 1)/framerate;
dRdt = sum(dRs)/dt;
```

B Nomenclature

A	Amplitude	[m]
c_L[1]	Concentration of dissolved CO_2 in liquid bulk	[mol/m^3]
c_0	Concentration in equilibrium with $P_{CO_2} = 1$ atm	[mol/m^3]
Δc	Concentration difference between the liquid bulk and the bubble	[J]
D	Diffusion coefficient	[m^2/s]
g	Acceleration due to gravity	[m/s^2]
ΔH_{diss}	Dissolution enthalpy of CO_2 in water	[J]
f	Frequency	[Hz]
k_H[1]	Henry's constant	[mol/m$^3 \cdot$Pa]
k_H°	Henry's constant at 298.15 K	[mol/m$^3 \cdot$Pa]
n[1]	Amount of substance	[mol]
P_{atm}	Atmospheric pressure	[Pa]
P_{CO_2}	Partial pressure of CO_2 above liquid	[Pa]
R	Radius	[m]
$\mathcal{R}$	Universal gas constant	[J/mol $\cdot$ K]
SR	Saturation ratio	[-]
SSR	Supersaturation ratio	[-]
t	Time	[s]
T	Temperature	[K]
v	Rising velocity	[m/s]
V	Volume	[m^3]
V_{head}	Volume of the headspace of a bottle of Spa Red	[m^3]
V_L	Volume of the liquid bulk	[m^3]

[1]Subscript i is used for the initial conditions, subscript e is used for the conditions at the time of the experiment

α	Numerical prefactor	[-]
γ	Surface tension	[N/m]
η	Viscosity	[Pa · s]
κ_{rest}	Radius growth rate constant for a bubble at rest	[m^2/s]
κ_{rising}	Radius growth rate constant for a rising bubble	[m/s]
ρ	Density	[kg/m^3]
ρ_{CO_2}	Density of CO_2	[kg/m^3]